AIMS Mathematics, 11(5): 14121–14140.
DOI: 10.3934/math.2026580
Received: 10 March 2026
Revised: 22 April 2026
Accepted: 07 May 2026
Published: 19 May 2026

https://www.aimspress.com/journal/Math

Research article

Statistical properties and inference for a new bounded lifetime model with application

Naelah Alghufily[1], Khalaf S. Sultan[2], Mahmoud M. M. Mansour[3,*] and Nagwa M. Mohamed[4]

[1] Department of Mathematical Sciences, College of Science, Princess Nourah Bint Abdulrahman University, P.O. Box 84428, Riyadh 11671, Saudi Arabia
[2] Mathematics Department, Faculty of Science, Al-Azhar University, Nasr City, P. O. Box 11884, Cairo, Egypt
[3] Department of Basic Science, Faculty of Engineering, The British University in Egypt, El Sherouk City, Cairo, Egypt
[4] Department of Mathematics and Computer Sceince, Faculty of Science, Suez University, P.O. Box 43221, Suez, Egypt

* **Correspondence:** Email: mahmoud.mansour@bue.edu.eg.

Abstract: A new two-parameter distribution on the unit interval $(0, 1)$ that is used to model bounded lifetime and reliability data is reported in this paper. The model is developed based on a transformation-based process and has the ability to support flexible shapes of hazard rates, including bathtub behavior. Basic properties like moments, entropy measures, and order statistics are obtained. The estimation of the parameter is formulated by the maximum likelihood and Bayesian estimation, and Bayesian inference is based on the Markov Chain Monte Carlo model. The performance of estimators is evaluated by simulation. The model is fitted to unit distributions of normalized failure-time data of 50 devices in an experiment of life-testing, showing competitive good-of-fit to existing unit distributions. The new framework is a dynamic instrument that can be used to analyze data on unit-interval lifetimes.

Keywords: unit-interval distribution; reliability analysis; bathtub-shaped hazard rate; Bayesian estimation; Markov chain Monte Carlo (MCMC)
Mathematics Subject Classification: 60E05, 62E10, 62F15, 62N05, 62P30

1. Introduction

The modeling of data with values in the unit interval $(0, 1)$ has gained importance because proportions, normalized lifetimes, and limited indices of reliability commonly occur in engineering, economics, medicine, and environmental sciences. Although classical bounded distributions, e.g.,

the Beta and Kumaraswamy families, are popular, they may not be sufficiently flexible in following complicated reliability patterns. In order to deal with this problem, alternative unit distributions have been suggested. As an example, Mazucheli et al. [1] came up with Unit-Weibull distribution as a versatile representation of bounded data, inspiring additional studies on Weibull-like constructions on the unit interval.

New bounded lifetime models are being developed alongside advances in computational inference. Bayesian estimation techniques, especially Markov chain Monte Carlo (MCMC) techniques, have become vital in cases when there is no closed-form solution available. Teirney [2] developed the basic structure of MCMC procedures that allow the exploration of posterior distributions of complex models efficiently.

Hazard rate behavior is one of the key elements in reliability analysis. Aarset [3] emphasized the significance of locating bathtub-shaped functions of hazards, which are usually found in mechanical systems. The most recent literature, like Gonzalez-Hernandez et al. [4], further states the need to have flexible models with bounds that can be applied to lifetime data. Other extensions encompass the unit-Weibull model that was investigated by Mazucheli et al. [5], such as the unit inverse Weibull distribution (UIWD) used by Ribeiro-Reis [6]. It is based on such developments that this paper proposes the unit Arcsine-Weibull distribution (UASWD), a two-parameter bounded model derived as a result of exponential transformation of the arcsine-Weibull generator. The proposed distribution has tractable formulas for its cumulative distribution, density, survival, and hazard functions and may have bathtub-shaped hazard behavior, thus being appropriate to normalized reliability data.

The UASWD can be applied to failure-time data that was initially reported by Aarset [3], which are the lifetimes of 50 devices. Due to the fact that the theoretical support of the model is (0, 1), the data are normalized in min-max before analysis. The results of comparative goodness-of-fit indicate that the UASWD performs better in comparison to rival unit distributions, such as Mazucheli et al. [1] and Ribeiro-Reis [6]. Both the maximum likelihood and Bayesian estimation procedures are devised. Bayesian inference is performed using MCMC routines according to Tierney [2], and a Monte Carlo simulation experiment compares the performance of different estimators in aspects of bias, mean square error, and interval coverage. This work has made a primary contribution, which can be summarized as follows. To begin with, a novel unit-bounded distribution, called the UASWD, is presented based on a transformation construction, which offers a versatile method of modeling data on the interval (0,1). Second, the proposed model can model a large variety of shapes of hazard rates, such as the significant bathtub behavior often seen in reliability analysis. Third, the distribution has a number of statistical properties, derived in closed form, such as moments, entropy measures, and order statistics. Fourth, both classical and Bayesian inference procedures are developed, where Bayesian estimation is implemented via MCMC techniques. Lastly, a detailed simulation study and an application to real data confirm the effectiveness and applicability of the proposed model as it demonstrates competitive performance with current unit distributions.

The rest of the paper is structured in the following way. Section 2 presents the distribution proposed and its properties. The primary statistical characteristics are obtained in Section 3. Estimation procedures are given in Section 4. Results of the simulation are reported in Section 5. Section 6 reports the application of the model on the normalized failure-time data in comparison with current distributions of units. Section 7 concludes the paper.

2. Unit arcsine-Weibull distribution

Let X be an arcsine-Weibull distribution (ASWD) with a cumulative distribution (CDF) function:

$$F_X(x) = \frac{2}{\pi}\sin^{-1}\left(\sqrt{1-e^{-(x/\lambda)^k}}\right), \quad x > 0,\ \lambda, k > 0. \tag{2.1}$$

Using the monotonic decreasing transformation $Y = e^{-X}$, we may create a unit-bounded distribution from the ASWD. Since $X \in (0,\infty)$, $Y \in (0,1)$, and $X = -logY$ is the inverse transformation, then the CDF is given as

$$G(y) = P_r(Y \le y) = P_r(e^{-X} \le y) = P_r(X \ge -\ln y) = 1 - F_X(-\ln y). \tag{2.2}$$

Substituting Eq (2.2) into Eq (2.1), we obtain the CDF as follows:

$$G(y) = 1 - \frac{2}{\pi}\sin^{-1}\left(\sqrt{1-e^{-(-\ln y/\lambda)^k}}\right), \quad 0 < y < 1. \tag{2.3}$$

This defines the UASWD. The probability density function (PDF) of UASWD is given by $g(y)$:

$$g(y) = \frac{k}{\pi\lambda y}\frac{\left(\frac{-\ln y}{\lambda}\right)^{k-1}\sqrt{e^{\left[-\left(\frac{-\ln y}{\lambda}\right)^k\right]}}}{\sqrt{1-e^{\left[-\left(\frac{-\ln y}{\lambda}\right)^k\right]}}}, \quad 0 < y < 1. \tag{2.4}$$

Using the transformation $u = \exp\left[-\left(\frac{-\ln y}{\lambda}\right)^k\right], du = \frac{ky^{-1}}{\lambda}\left(\frac{-lny}{\lambda}\right)^{k-1} exp\left[-\left(\frac{-lny}{\lambda}\right)^k\right]dy$; then, $\frac{1}{\pi}\int_0^1 \frac{du}{\sqrt{u(1-u)}} = \frac{1}{\pi}B(\frac{1}{2},\frac{1}{2})$, where $B(m,n)$ is beta function.

It follows that $\int_0^1 g(y)\,dy = 1$, confirming that $g(y)$ is a valid PDF. The survival function is given by

$$R(y) = 1 - G(y) = \frac{2}{\pi}\sin^{-1}\left(\sqrt{1-e^{\left[-\left(\frac{-\ln y}{\lambda}\right)^k\right]}}\right). \tag{2.5}$$

The hazard rate function is

$$H(y) = \frac{g(y)}{R(y)} = \frac{k\left(\frac{-lny}{\lambda}\right)^{k-1}\sqrt{e^{\left[-\left(\frac{-\ln y}{\lambda}\right)^k\right]}}}{2\lambda y\sqrt{\left[1-e^{-\left(\frac{-\ln y}{\lambda}\right)^k}\right]}\sin^{-1}\left(\sqrt{1-e^{\left[-\left(\frac{-\ln y}{\lambda}\right)^k\right]}}\right)}. \tag{2.6}$$

Figures 1 and 2 present the shapes of $H(y)$ and $R(y)$ for the UASWD. The behavior of the hazard function $H(y)$ for various values of the parameter k is shown in Figure 1. The curves show a bathtub-shaped pattern with an initially declining hazard rate, a practically constant region, and an increasing trend for higher y values. The behavior of the reliability function $R(y)$ for a range of parameter k values is depicted in Figure 2. It proves that the reliability function is a decreasing function of y, which is in agreement with the basic characteristic of reliability functions.

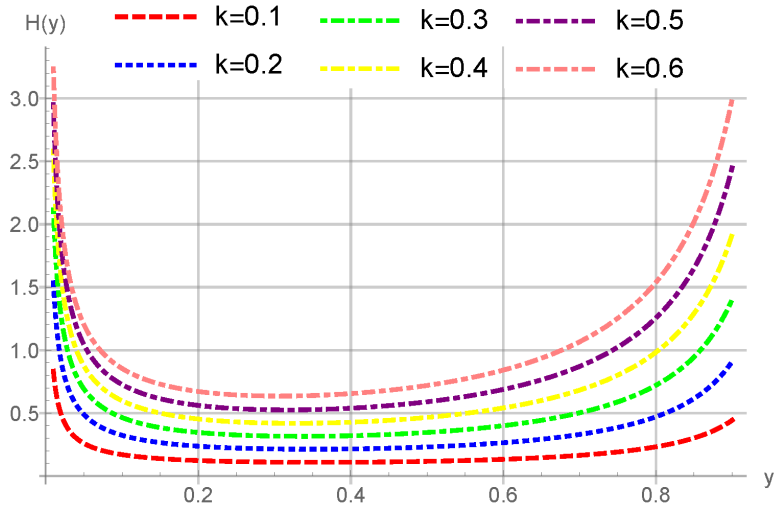

Figure 1. $H(y)$ for different values of k.

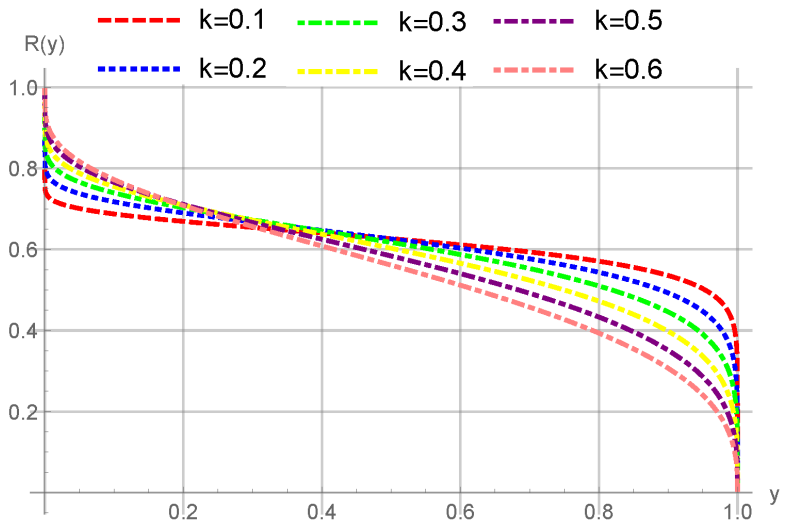

Figure 2. $R(y)$ for different values of k.

3. Statistical properties

In this section, some of the distributional properties of UASWD, including the quantile function, the moments, the moment-generating function, Rényi entropy, order statistics, the odds function, and Shannon entropy, are derived.

3.1. Quantile function

The main significance of the quantile function is seen in inverse transform sampling, which is the basic technique for utilizing a computer to generate random numbers from any statistical distribution. It also serves as the mathematical basis for risk management, providing a thorough understanding of a distribution through significant percentiles (median, quartiles) and directly defining measurements like value at risk in finance. By focusing on probabilities rather than values, it offers a solid basis

for comparing statistics, identifying outliers, and modeling real-world systems. The definition of the quantile function is the real solution of Eq (3.1) as follows:

$$G(y_q) = u, \qquad 0 \leq q \leq 1. \tag{3.1}$$

Then,

$$y_q = \exp\left[-\lambda\left[-\log\left(1 - \sin^2\left(\frac{\pi}{2}\left(1 - u\right)\right)\right)\right]^{\frac{1}{k}}\right]. \tag{3.2}$$

3.2. Moments

In probability and statistics, moments are important numerical measurements that describe distributions. While the second moment (variance) evaluates data spread, the first moment (mean) determines central location. Asymmetry is indicated by the third moment (skewness), and the likelihood of an outlier is suggested by the fourth moment (kurtosis), which is related to tail heaviness. Additionally, moments are necessary for the creation of moment-generating functions that define probability distributions and for parameter estimation using the method of moments. They provide a basic framework for calculating uncertainty and drawing conclusions from statistics.

The r-th moment for UASWD is

$$\mu_r^{'} = E(Y^r) = \int_0^1 y^r g(y) dy = \frac{k}{\pi\lambda}\int_0^1 y^{r-1}\frac{\left(-\frac{\ln y}{\lambda}\right)^{k-1}\sqrt{e^{-\left(-\frac{\ln y}{\lambda}\right)^k}}}{\sqrt{1 - e^{-\left(-\frac{\ln y}{\lambda}\right)^k}}} dy. \tag{3.3}$$

Using the transformation $u = \left(-\frac{\ln y}{\lambda}\right)^k, du = -\frac{k}{\lambda}u^{1-\frac{1}{k}}e^{\lambda u^{\frac{1}{k}}}dy$, the integral becomes

$$\mu_r^{'} = \frac{1}{\pi}\int_0^{\infty}\frac{e^{-r\lambda u^{\frac{1}{k}}}e^{-\frac{u}{2}}}{\sqrt{1 - e^{-u}}} du. \tag{3.4}$$

Using the series expansion for $e^{-r\lambda u^{\frac{1}{k}}}$ and $\sqrt{1 - e^{-u}}$, we get

$$e^{-r\lambda u^{\frac{1}{k}}} = \sum_{n=0}^{\infty}(-1)^n\frac{(r\lambda)^n}{n!}u^{\frac{n}{k}}, \tag{3.5}$$

$$\sqrt{1 - e^{-u}} = \sum_{m=0}^{\infty}\frac{\binom{2m}{m}}{4^m}e^{-mu}, \tag{3.6}$$

and then by using Eqs (3.5) and (3.6) in Eq (3.4), we obtain

$$\mu_r^{'} = \frac{1}{\pi}\sum_{n=0}^{\infty}(-1)^n\frac{(r\lambda)^n}{n!}\sum_{m=0}^{\infty}\frac{\binom{2m}{m}}{4^m}\int_0^{\infty}u^{\frac{n}{k}}e^{-\left(m+\frac{1}{2}\right)u}du. \tag{3.7}$$

Recognizing this integral as the Gamma function $\Gamma(a) = \int_0^{\infty}u^{a-1}e^{-u}du$, and after some simplifications, we get

$$\mu_r^{'} = \frac{1}{\pi}\sum_{n=0}^{\infty}(-1)^n\frac{(r\lambda)^n}{n!}\sum_{m=0}^{\infty}\frac{\binom{2m}{m}}{4^m}\frac{\Gamma(\frac{n}{k}+1)}{(m+\frac{1}{2})^{\frac{n}{k}+1}}. \tag{3.8}$$

3.3. Moment-generating function

The moment-generating function (MGF) is an effective tool that makes statistical mathematical operations easier and provides a unique description of a probability distribution. Its capacity to produce all moments (mean, variance, etc.) through straightforward differentiation, as opposed to intricate integration, is what makes it so significant. The moment-generating function for UASWD is defined as:

$$M_Y(t) = E(e^{tY}) = \frac{k}{\pi\lambda}\int_0^1 y^{-1}\frac{e^{ty}\left(-\frac{\ln y}{\lambda}\right)^{k-1}\sqrt{e^{-\left(-\frac{\ln y}{\lambda}\right)^k}}}{\sqrt{1-e^{-\left(-\frac{\ln y}{\lambda}\right)^k}}}dy. \tag{3.9}$$

Using the transformation $u = \left(-\frac{\ln y}{\lambda}\right)^k, du = -\frac{k}{\lambda}u^{1-\frac{1}{k}}e^{\lambda u^{\frac{1}{k}}}dy$ and changing the limits of integration, the integral becomes

$$M_Y(t) = \frac{1}{\pi}\int_0^\infty \frac{e^{-\lambda t u^{\frac{1}{k}}-\frac{u}{2}}}{\sqrt{1-e^{-u}}}du. \tag{3.10}$$

Using the series expansion for $e^{-r\lambda u^{\frac{1}{k}}}$ and $\sqrt{1-e^{-u}}$ as in Eq (3.5) and Eq (3.6), we obtain

$$M_Y(t) = \frac{1}{\pi}\sum_{n=0}^\infty \frac{t^n}{n!}\sum_{r=0}^\infty (-1)^r\frac{(n\lambda)^r}{r!}\sum_{m=0}^\infty \frac{\binom{2m}{m}}{4^m}\int_0^\infty u^{\frac{r}{k}}e^{-(m+\frac{1}{2})u}du. \tag{3.11}$$

Using the Gamma function, $\Gamma(a) = \int_0^\infty u^{a-1}e^{-u}du$, and after some simplifications, we get

$$M_Y(t) = \frac{1}{\pi}\sum_{n=0}^\infty \frac{t^n}{n!}\sum_{r=0}^\infty (-1)^r\frac{(n\lambda)^r}{r!}\sum_{m=0}^\infty \frac{\binom{2m}{m}}{4^m}\frac{\Gamma(\frac{r}{k}+1)}{\left(m+\frac{1}{2}\right)^{(\frac{r}{k}+1)}}. \tag{3.12}$$

3.4. Rényi entropy

A strong parametric framework for measuring uncertainty, information, and distributional disparity is provided by Rényi entropy. In order to measure uncertainty in lifetime distributions and residual life of systems and components, Rényi entropy is essential. Engineers can evaluate how unpredictability increases as a system ages using its dynamic forms, including residual Rényi entropy, which provides insights into failure behavior and aging features. Sensitivity tuning is made possible by the parameter p, where high values highlight usual working life and low values highlight uncommon failure events in the tail. Based on maximum entropy principles, it is used to characterize and choose suitable lifetime models. Moreover, failure data is analyzed, system reliability is evaluated, and models are validated against actual component failure times using Rényi based measures. For more details, see Xing [7] and Kumar [8].

The Rényi entropy of order $p > 0, p \neq 1$ is defined as

$$R_p(Y) = \frac{1}{1-p}\log\left[\int_0^1 \frac{k}{\pi\lambda y}\frac{\left(-\frac{\ln y}{\lambda}\right)^{k-1}\sqrt{e^{-\left(-\frac{\ln y}{\lambda}\right)^k}}}{\sqrt{1-e^{-\left(-\frac{\ln y}{\lambda}\right)^k}}}\right]^p dy = \frac{1}{1-p}\log\left[\frac{k}{\pi\lambda}\right]^p I_P, \tag{3.13}$$

where

$$I_P = \int_0^1 y^{-p} \frac{\left(-\frac{\ln y}{\lambda}\right)^{p(k-1)} e^{-\frac{p}{2}\left(-\frac{\ln y}{\lambda}\right)^k}}{\left(1 - e^{-\left(-\frac{\ln y}{\lambda}\right)^k}\right)^{\frac{p}{2}}} dy. \tag{3.14}$$

Using the transfomation $t = \left(-\frac{\ln y}{\lambda}\right)^k, dt = -\frac{k}{\lambda} u^{1-\frac{1}{k}} e^{\lambda u^{\frac{1}{k}}} dy$, and changing the limits of integration, we have,

$$I_P = \frac{\lambda}{k} \int_0^\infty t^{\frac{p(k-1)}{k} + \frac{1}{k} - 1} \frac{e^{-\frac{p}{2}t} e^{(p-1)\lambda t^{\frac{1}{k}}}}{(1 - e^{-t})^{\frac{p}{2}}} dt. \tag{3.15}$$

Using the series expansion for $e^{(p-1)\lambda t^{\frac{1}{k}}}$ and $(1 - e^{-t})^{-\frac{p}{2}}$, we get the following:

$$e^{(p-1)\lambda t^{\frac{1}{k}}} = \sum_{m=0}^{\infty} \frac{[(p-1)\lambda]^m}{m!} t^{\frac{m}{k}}, \tag{3.16}$$

$$(1 - e^{-t})^{-\frac{p}{2}} = \sum_{j=0}^{\infty} \binom{\frac{p}{2} + j - 1}{j} e^{-jt}. \tag{3.17}$$

By substituting Eqs (3.16) and (3.17) into Eq (3.15), we obtain

$$I_P = \frac{\lambda}{k} \sum_{j=0}^{\infty} \binom{\frac{p}{2} + j - 1}{j} \sum_{m=0}^{\infty} \frac{[(p-1)\lambda]^m}{m!} \int_0^\infty t^{\frac{m}{k} + \frac{p(k-1)}{k} + \frac{1}{k} - 1} e^{-\left(\frac{p}{2} + j\right)t} dt. \tag{3.18}$$

Using the Gamma function $\Gamma(a) = \int_0^\infty u^{a-1} e^{-u} du$,, and after some simplifications, we obtain

$$I_P = \frac{\lambda}{k} \sum_{j=0}^{\infty} \binom{\frac{p}{2} + j - 1}{j} \sum_{m=0}^{\infty} \frac{[(p-1)\lambda]^m}{m!} \frac{\Gamma\left(\frac{m}{k} + \frac{p(k-1)}{k} + \frac{1}{k}\right)}{\left(\frac{p}{2} + j\right)^{\left(\frac{m}{k} + \frac{p(k-1)}{k} + \frac{1}{k}\right)}}. \tag{3.19}$$

By substituting Eq (3.19) into Eq (3.13), we obtain the Rényi entropy.

3.5. Order statistics

Let (Y_1, Y_n) represent the order statistics of minimum and maximum ranks from the UASWD. The PDFs for $i - th$ order statistics are given by:

$$g_{k:n} = \frac{n!}{(k-1)!(n-k)!} g(y) [G(y)]^{k-1} [1 - G(y)]^{n-k}, \qquad k = 1, 2, \cdots, n.$$

The PDF of the minimum order statistic $Y_{(1)}$ is

$$g_{1:n} = n [1 - G(y)]^{n-1} g(y),$$

so then,

$$g_{1:n} = \frac{nk}{\pi\lambda y} \left[\frac{2}{\pi} \sin^{-1}\left(\sqrt{1 - e^{-\left(-\frac{\ln y}{\lambda}\right)^k}}\right)\right]^{n-1} \frac{\left(-\frac{\ln y}{\lambda}\right)^{k-1} \sqrt{e^{-\left(-\frac{\ln y}{\lambda}\right)^k}}}{\sqrt{1 - e^{-\left(-\frac{\ln y}{\lambda}\right)^k}}}.$$

Also, The PDF of the maximum order statistic $Y_{(n)}$ is

$$g_{n:n} = n\left[G(y)\right]^{n-1} g(y),$$

$$g_{n:n} = \frac{nk}{\pi\lambda y}\left[1 - \frac{2}{\pi}\sin^{-1}\left(\sqrt{1 - e^{-\left(-\frac{\ln y}{\lambda}\right)^k}}\right)\right]^{n-1} \frac{\left(-\frac{\ln y}{\lambda}\right)^{k-1}\sqrt{e^{-\left(-\frac{\ln y}{\lambda}\right)^k}}}{\sqrt{1 - e^{-\left(-\frac{\ln y}{\lambda}\right)^k}}}.$$

For more details on order statistics, see Arnold [9].

3.6. Odds function

The odds function is defined to be the ratio of the CDF to the survival function $R(y)$ as follows:

$$O(y;\lambda,k) = \frac{G(y)}{R(y)} = \frac{1 - \frac{2}{\pi}\sin^{-1}\left(\sqrt{1 - e^{-(-\frac{\ln y}{\lambda})^k}}\right)}{\frac{2}{\pi}\sin^{-1}\left(\sqrt{1 - e^{-(-\frac{\ln y}{\lambda})^k}}\right)}.$$

The odds function is a crucial tool in reliability engineering for examining failure behavior over time. Because its derivative with respect to time yields the hazard rate, it gives engineers a direct measure of the instantaneous propensity to fail and enables them to model how risk changes over the course of a product's life cycle. The proportional odds model, a potent semi parametric method for comparing the effects of various stress factors or manufacturing conditions on failure times, is based on this function.

Furthermore, a logistic distribution for the lifetime is indicated when the log-odds (logit) of failure shows a linear relationship with time. This is especially helpful for modeling accelerated life tests and early failure periods. In the final analysis, this approach helps engineers to optimize maintenance plans by evaluating the compromise between the costs of preventive replacement and the growing chances of failure. For more details, see Nair et al. [10].

3.7. Shannon entropy

The Shannon entropy for a continuous random variable $Y$is defined as follows:

$$S_h(k,\lambda) = -\int_0^1 g(y)\ln g(y)dy,$$

so then,

$$S_h(k,\lambda) = -\int_0^1 \frac{k}{\pi\lambda y}\frac{\left(-\frac{\ln y}{\lambda}\right)^{k-1}\sqrt{e^{-\left(-\frac{\ln y}{\lambda}\right)^k}}}{\sqrt{1 - e^{-\left(-\frac{\ln y}{\lambda}\right)^k}}}\ln\left(\frac{k}{\pi\lambda y}\frac{\left(-\frac{\ln y}{\lambda}\right)^{k-1}\sqrt{e^{-\left(-\frac{\ln y}{\lambda}\right)^k}}}{\sqrt{1 - e^{-\left(-\frac{\ln y}{\lambda}\right)^k}}}\right)dy.$$

Shannon entropy is a foundational concept because it provides a universal measure of uncertainty, information content, and complexity that applies across virtually every field of science and engineering. At its core, entropy quantifies how much "surprise" or "information" is contained in an outcome: Low entropy means predictability and order, while high entropy means randomness and uncertainty. Shannon entropy is crucial in reliability engineering because it quantifies the uncertainty and

unpredictability of failure times, something traditional metrics like mean time before failure cannot capture. A component with low entropy fails predictably within a narrow time window (e.g., wear-out), while high entropy indicates random, unpredictable failures. This distinction matters for two practical reasons: model selection and health monitoring. When data is limited, the principle of maximum entropy guides engineers to choose the least biased failure distribution (e.g., the exponential distribution for constant failure rates). Additionally, tracking entropy over time from sensor data (vibration, acoustics) reveals increasing system disorder, serving as an early warning signal for impending failure. Thus, entropy helps engineers select honest statistical models, detect degradation early, and choose appropriate maintenance strategies based on how predictable or random the failure behavior truly is. For more details, see Kumar [8].

4. Parameters estimation

This section outlines the parameter estimation methods employed: maximum likelihood estimation (MLE) and the Bayesian approach.

4.1. Maximum likelihood estimation

Let $X_1, X_2, ..., X_n$ be a random sample from the UASWD with observed values $x_1, x_2, ..., x_n$, then, the likelihood function of the sample is

$$L(\lambda, k) = \prod_{i=1}^{n} g(y_i) = \left(\frac{k}{\pi\lambda}\right)^n \prod_{i=1}^{n} \frac{\left(\frac{-\ln y_i}{\lambda}\right)^{k-1} \sqrt{\exp\left[-\left(\frac{-\ln y_i}{\lambda}\right)^k\right]}}{\sqrt{\left[1-\exp\left(-\left(\frac{-\ln y_i}{\lambda}\right)^k\right)\right]}}. \tag{4.1}$$

The log likelihood function of this sample is

$$l(\lambda, k) = n\ln k - n\ln(\pi\lambda) + (k-1)\ln\left(\sum_{i=1}^{n} -\frac{\ln y_i}{\lambda}\right) - \frac{1}{2}\sum_{i=1}^{n}\left(-\frac{\ln y_i}{\lambda}\right)^k - \frac{1}{2}\sum_{i=1}^{n}\ln\left[1-exp\left(-\left(-\frac{\ln y_i}{\lambda}\right)^k\right)\right], \tag{4.2}$$

where the quantity $z_i = -\frac{\ln y_i}{\lambda} > 0$, $0 < y_i < 1$ and , $\lambda > 0$.

Upon differentiating Eq (4.2) with respect to k and λ, we obtain

$$\frac{\partial\ell(\lambda, k)}{\partial k} = -\frac{1}{2}\sum_{i=1}^{n}\frac{\ln(z_i)\, e^{-z_i^k} z_i^k}{1-e^{-z_i^k}} - \frac{1}{2}\sum_{i=1}^{n}\ln(z_i)\, z_i^k + \ln\left(\sum_{i=1}^{n} z_i\right) + \frac{n}{k}, \tag{4.3}$$

$$\frac{\partial\ell(\lambda, k)}{\partial\lambda} = -\frac{1}{2}\sum_{i=1}^{n}\frac{k\,\ln(y_i)\, z_i^{k-1}}{\lambda^2} + \frac{(k-1)\sum_{i=1}^{n}\frac{\ln(y_i)}{\lambda^2}}{\sum_{i=1}^{n} z_i} - \frac{1}{2}\sum_{i=1}^{n}\frac{k\,\ln(y_i)\, e^{-z_i^k} z_i^{k-1}}{\lambda^2\left(1-e^{-z_i^k}\right)} - \frac{n}{\lambda}. \tag{4.4}$$

A system of nonlinear simultaneous Eqs (4.3) and (4.4) in two unknown variables k and λ resulted. It is obvious that a solution is not easy to reach. Therefore, a method such as Newton-Raphson iteration can be used to find an approximate solution of the preceding nonlinear system; details about the algorithm for implementing Newton-Raphson iterations can be referred to in Burden and Faires [11].

We can then get $\hat{k}$ and $\hat{\lambda}$. Mathematica software, version 12, has been used to apply the Newton-Raphson algorithm via a command called "FindRoot", as applying this command guarantees stable convergence for getting the approximate solution. More details about the "FindRoot" command are available via the following URL: https://reference.wolfram.com/language/ref/FindRoot.html, accessed on 25 February 2026.

Set up $(1-\delta)\%$ approximate confidence intervals for the parameters k and λ of the form

$$(\hat{k}_L, \hat{k}_U) = \hat{k} \pm z_{\frac{\alpha}{2}} \sqrt{var(\hat{k})}, (\hat{\lambda}_L, \hat{\lambda}_U) = \hat{\lambda} \pm z_{\frac{\alpha}{2}} \sqrt{var(\hat{\lambda})}, \tag{4.5}$$

where $z_{\frac{\alpha}{2}}$ is the percentile of the standard normal distribution with left-tail probability $\frac{\delta}{2}$, and $var(\hat{k})$ and $var(\hat{\lambda})$ represent the asymptotic variance of maximum likelihood estimates, which can be calculated using the inverse of the Fisher information matrix; for more details see Cohen [12]. The asymptotic variance-covariance matrix for the maximum likelihood estimates can be written as follows:

$$F^{-1} = \begin{bmatrix} -\frac{\partial^2 l(k,\lambda)}{\partial k^2} & -\frac{\partial^2 l(k,\lambda)}{\partial k \partial \lambda} \\ -\frac{\partial^2 l(k,\lambda)}{\partial \lambda \partial k} & -\frac{\partial^2 l(k,\lambda)}{\partial \lambda^2} \end{bmatrix}^{-1}_{\downarrow(\hat{k},\hat{\lambda})} = \begin{bmatrix} var(\hat{k}) & cov(\hat{k}\hat{\lambda}) \\ cov(\hat{\lambda}\hat{k}) & var(\hat{\lambda}) \end{bmatrix},$$

where the second partial derivatives of the log likelihood function can be derived as follows:

$$\frac{\partial^2 \ell(\lambda,k)}{\partial k^2} = -\frac{n}{k^2} - \frac{1}{2}\sum_{i=1}^{n}\left[\frac{\ln^2(z_i)\, e^{-z_i^k} z_i^k}{1-e^{-z_i^k}} - \frac{\ln^2(z_i)\, e^{-z_i^k} z_i^{2k}}{1-e^{-z_i^k}} - \frac{\ln^2(z_i)\, e^{-2z_i^k} z_i^{2k}}{\left(1-e^{-z_i^k}\right)^2}\right] - \frac{1}{2}\sum_{i=1}^{n}\ln^2(z_i)\, z_i^k, \tag{4.6}$$

$$\begin{aligned}\frac{\partial^2 \ell(\lambda,k)}{\partial \lambda^2} =& -\frac{1}{2}\sum_{i=1}^{n}\left[-\frac{k^2\ln^2(y_i)\, e^{-z_i^k} z_i^{2k-2}}{\lambda^4\left(1-e^{-z_i^k}\right)} - \frac{k^2\ln^2(y_i)\, e^{-2z_i^k} z_i^{2k-2}}{\lambda^4\left(1-e^{-z_i^k}\right)^2}\right.\\ &\left. - \frac{2k\ln(y_i)\, e^{-z_i^k} z_i^{k-1}}{\lambda^3\left(1-e^{-z_i^k}\right)} + \frac{k\ln(y_i)\, e^{-z_i^k}}{\lambda^2\left(1-e^{-z_i^k}\right)}\left(\frac{k\ln(y_i)\, z_i^{k-2}}{\lambda^2} - \frac{\ln(y_i)\, z_i^{k-2}}{\lambda^2}\right)\right]\\ &+ \frac{(k-1)\sum_{i=1}^{n}\left(-\frac{2\ln(y_i)}{\lambda^3}\right)}{\sum_{i=1}^{n} z_i} - \frac{(k-1)\left(\sum_{i=1}^{n}\frac{\ln(y_i)}{\lambda^2}\right)^2}{\left(\sum_{i=1}^{n} z_i\right)^2}\\ &- \frac{1}{2}\sum_{i=1}^{n}\left[\frac{k\ln(y_i)}{\lambda^2}\left(\frac{k\ln(y_i)\, z_i^{k-2}}{\lambda^2} - \frac{\ln(y_i)\, z_i^{k-2}}{\lambda^2}\right) - \frac{2k\ln(y_i)\, z_i^{k-1}}{\lambda^3}\right] + \frac{n}{\lambda^2},\end{aligned} \tag{4.7}$$

$$\begin{aligned}\frac{\partial^2 \ell(\lambda,k)}{\partial \lambda\, \partial k} =& -\frac{1}{2}\sum_{i=1}^{n}\left(\frac{k\ \ln(y_i)\ \ln(z_i)\, z_i^{k-1}}{\lambda^2} - \frac{z_i^k}{\lambda}\right)\\ &- \frac{1}{2}\sum_{i=1}^{n}\left[\frac{k\ \ln(y_i)\ \ln(z_i)\, e^{-z_i^k} z_i^{k-1}}{\lambda^2\left(1-e^{-z_i^k}\right)} - \frac{k\ \ln(y_i)\ \ln(z_i)\, e^{-z_i^k} z_i^{2k-1}}{\lambda^2\left(1-e^{-z_i^k}\right)}\right.\\ &\left. - \frac{k\ \ln(y_i)\ \ln(z_i)\, e^{-2z_i^k} z_i^{2k-1}}{\lambda^2\left(1-e^{-z_i^k}\right)^2} - \frac{e^{-z_i^k} z_i^k}{\lambda\left(1-e^{-z_i^k}\right)}\right] + \frac{\sum_{i=1}^{n}\frac{\ln(y_i)}{\lambda^2}}{\sum_{i=1}^{n} z_i}.\end{aligned} \tag{4.8}$$

By substituting Eqs (4.6)–(4.8) into F^{-1} and using Eq (4.5), $(1-\delta)\%$ approximate confidence intervals for the parameters k and λ are obtained.

4.2. Bayesian estimation

The prominence of Bayesian estimation has grown considerably in recent years, establishing it as a crucial tool for addressing diverse challenges across numerous scientific and engineering domains. To infer meaningful insights from observed data, practitioners frequently utilize non-Bayesian frameworks, with maximum likelihood estimation serving as a prime example. This methodological duality is applied extensively in fields as varied as statistics, econometrics, and biostatistics and extends into technological areas such as speech and image processing, computer vision, and astronomy. Its reach further encompasses telecommunications, the development of neural networks, pattern recognition, machine learning, and artificial intelligence, underscoring its fundamental role in modern data analysis. The joint prior of the parameters k and λ can be written as $\pi_1(k) = k^{a_1-1}e^{-b_1 k}, \pi_2(\lambda) = \lambda^{a_2-1}e^{-b_2\lambda}, k > 0$, and $\lambda > 0$.

The reason behind the choice of gamma prior distributions on the parameters k and λ is that they are flexible and suitable for modeling positive-valued quantities, a general convention in Bayesian reliability analysis. The hyperparameters in this paper are selected to be small, which implies weakly informative priors that have a negligible impact on the posterior distribution. The option enables the observed data to assume a more predominant role in the inference process and gives a broad outline of how to assess the performance of the proposed estimators without placing any stringent prior assumptions.

The joint posterior density function of k and λ denoted by $\pi^*(k, \lambda|\underline{t})$ can be written as

$$\pi^*(k, \lambda|\underline{t}) = \frac{L(k, \lambda) \times \pi(k, \lambda)}{\int_0^\infty \int_0^\infty L(k, \lambda) \times \pi(k, \lambda) dk d\lambda}. \tag{4.9}$$

If φ is the parameter to be estimated by an estimator $\hat{\varphi}$, then the squared error loss (SEL) function is defined as

$$L(\varphi, \hat{\varphi}) = (\varphi - \hat{\varphi})^2,$$

and the Bayes estimate of any function of k and λ, say $g(k, \lambda)$, under the SEL function is

$$\hat{g}_{BS}(k, \lambda|\underline{x}) = E_{k,\lambda|\underline{x}}(g(k, \lambda)), \tag{4.10}$$

where

$$E_{k,\lambda,|\underline{x}}(g(k, \lambda)) = \frac{\int_0^\infty \int_0^\infty g(k, \lambda)\pi_1(k)\pi_2(\lambda)L(k, \lambda|\underline{x}) dk d\lambda}{\int_0^\infty \int_0^\infty \pi_1(k)\pi_2(\lambda)L(k, \lambda|\underline{x}) dk d\lambda}.$$

The Bayes estimate of $h(k, \lambda)$ using linear-exponential loss function (LINEX) is

$$\hat{h}_{BL}(\alpha, a, b, \theta) = \frac{-1}{c} \log\left[E_{k,\lambda|\underline{t}}\left[e^{-ch(k,\lambda)}\right]\right], \ c \neq 0, \tag{4.11}$$

where

$$E_{k,\lambda|\underline{t}}\left[e^{-ch(k,\lambda)}\right] = \frac{\int_0^\infty \int_0^\infty e^{-ch(k,\lambda)} \times L(k, \lambda) \times \pi(k, \lambda) dk d\lambda}{\int_0^\infty \int_0^\infty L(k, \lambda) \times \pi(k, \lambda) dk d\lambda}.$$

The c in the LINEX loss function is used to balance the asymmetry of estimation errors, with positive values indicating overestimation and negative ones referring to underestimation; see

Varian [13]. Practically, which error it picks up is a question of the relative cost of these errors. In this analysis, the representative value ($c = \pm 2$) is employed to depict its impact without imposing application-specific preferences.

From Eq (4.9), the conditional density posterior functions of k and λ are as follows:

$$\pi_1^*(k|\lambda,\underline{t}) \propto k^{n+a-1}e^{-bk}\prod_{i=1}^{n}\frac{\left(-\frac{\ln y_i}{\lambda}\right)^{k-1}\sqrt{e^{-\left(-\frac{\ln y_i}{\lambda}\right)^k}}}{\sqrt{1-e^{-\left(-\frac{\ln y_i}{\lambda}\right)^k}}}, \tag{4.12}$$

$$\pi_2^*(k|\lambda,\underline{t}) \propto \lambda^{-n+w-1}e^{-rk}\prod_{i=1}^{n}\frac{\left(-\frac{\ln y_i}{\lambda}\right)^{k-1}\sqrt{e^{-\left(-\frac{\ln y_i}{\lambda}\right)^k}}}{\sqrt{1-e^{-\left(-\frac{\ln y_i}{\lambda}\right)^k}}}. \tag{4.13}$$

Since the conditional posterior of k and λ in Eqs (4.12) and (4.13) do not present standard forms, the MCMC technique is used as follows:

(1) Start with $k^{(0)}$ and $\lambda^{(0)}$.

(2) Put $j = 1$.

(3) Using the following Metropolis-Hastings algorithm, generate $k^{(j)}$ and $\lambda^{(j)}$ from Eqs (4.12) and (4.13) with the normal suggested distribution $N\left(k^{(j-1)}, var(k)\right)$ and $N\left(\lambda^{(j-1)}, var(\lambda)\right)$, respectively, where $var(k)$ and $var(\lambda)$ can be obtained from the main diagonal in the inverse Fisher's information matrix.
(i) Generate a proposal k^* from $N\left(k^{(j-1)}, var(k)\right)$ and λ^* from $N\left(\lambda^{(j-1)}, var(\lambda)\right)$.
(ii) Evaluate the acceptance probabilities

$$\rho_k = \min\left[1, \frac{\pi_1^*(k^*|\lambda^{(j-1)},\underline{t})}{\pi_1^*(k^{(j-1)}|\lambda^{(j-1)},\underline{t})}\right], \qquad \rho_\lambda = \min\left[1, \frac{\pi_2^*(\lambda^*|k^{(j)},\underline{t})}{\pi_2^*(\lambda^{(j-1)}|k^{(j)},,\underline{t})}\right], \quad \Big\}.$$

(4) Compute $k^{(j)}$ and $\lambda^{(j)}$.

(5) Put $j = j + 1$.

(6) Repeat Steps 3-4 L times.

(7) To guarantee the convergence and to remove the influence of the selection of initial values, the first B simulated varieties are ignored. Then, the selected samples are $k^{(j)}$ and $\lambda^{(j)}$. $j = B + 1, ..., L$, for sufficiently large L, forms an approximate posterior samples which can be used to obtain the Bayes MCMC point estimates of $k^{(j)}$ and $\lambda^{(j)}$ as

$$\hat{k}_{MCMC} = \frac{1}{L-B}\sum_{j=B+1}^{L} k^{(j)}, \quad \hat{\lambda}_{MCMC} = \frac{1}{L-B}\sum_{j=B+1}^{L} \lambda^{(j)}, j = 1, 2. \tag{4.14}$$

(8) To calculate the credible interval (CRIs) of Ω_s where $\Omega_1 = k$ and $\Omega_2 = \lambda$. The quantiles of the samples can be evaluated as the endpoints of the interval. Sort $\left\{\Omega_s^{B+1}, \Omega_s^{B+2}, ..., \Omega_s^{L}\right\}$ as $\left\{\Omega_s^{[1]}, \Omega_s^{[2]}, ..., \Omega_s^{[L-B]}\right\}$. The $100(1-\tau)\%$ symmetric credible interval of Ω_s is

$$\left[\Omega_s(\frac{\tau}{2}(L-B), \Omega_s((1-\frac{\tau}{2})(L-B))\right]. \tag{4.15}$$

5. Simulation study

In this section, a comprehensive Monte Carlo simulation analysis was carried out to assess the effectiveness of various estimation techniques for the UASWD parameters under complete sampling. The simulation seeks to evaluate the accuracy and reliability of interval estimates, point estimates, and related characteristics for a variety of sample sizes. Mathematica software (version 12) was used to implement all computational methods.

The following indices are being taken into consideration when designing the simulation study: The parameters of the true parameters were set to $(k, \lambda) = (2, 0.5)$. The effectiveness of the various approaches to the resulting estimates of k and λ are compared in terms of their mean square errors (MSEs) and average length of confidence intervals (ALCIs) as well as the coverage probability (CP), which contains the true values of interest. While the asymptotic distributions of MLEs are used to obtain the asymptotic confidence intervals (ACIs). Sample sizes of $(n = 20, 40, 60, 80, 100)$ are included. We create a Markov chain with 100 observations by running the Gibbs sampler with the Metropolis-Hastening algorithm, as recommended by Teirney [2]. The first 10 values are discarded as "burn-in", and we employ informative gamma prior distributions with hyperparameters of $a_1 = 0.01, b_1 = 0.02, a_2 = 0.01$, and $b_2 = 0.02$.

Tables 1 and 2 display the results of various point estimates and MSE while Tables 3 and 4 display the results of ACIs and CPs of 95 percent.

Table 1. Bias and MSE values for $k = 2$.

n	MLE		SEL		LINEX			
					$c = -2$		$c = 2$	
	Bias	MSE	Bias	MSE	Bias	MSE	Bias	MSE
20	2.1508	0.2014	2.0082	0.0725	2.0244	0.0777	1.9926	0.0708
40	2.0727	0.0672	2.0081	0.0190	2.0145	0.0217	2.0020	0.0168
60	2.0540	0.0498	2.0030	0.0192	2.0050	0.0201	2.0009	0.0184
80	2.0508	0.0443	2.0052	0.0038	2.0069	0.0039	2.0036	0.0038
100	2.0182	0.0195	2.0120	0.0055	2.0124	0.0055	2.0117	0.0056

Table 2. Bias and MSE values for $\lambda = 0.5$.

n	MLE		SEL		LINEX			
					$c = -2$		$c = 2$	
	Bias	MSE	Bias	MSE	Bias	MSE	Bias	MSE
20	0.5004	0.0066	0.5051	0.0040	0.5064	0.0041	0.5039	0.0040
40	0.5060	0.0038	0.5013	0.0011	0.5017	0.0011	0.5009	0.0010
60	0.5060	0.0026	0.5027	0.0008	0.5029	0.0008	0.5025	0.0008
80	0.4996	0.0022	0.4994	0.0004	0.4995	0.0004	0.4993	0.0004
100	0.5009	0.0014	0.5026	0.0004	0.5026	0.0004	0.5026	0.0004

Table 3. ALCIs and CPs for $k = 2$.

n	95% ACI		95% CRI	
	ALCI	CP	ALCI	CP
20	1.6166	0.9550	1.3567	0.9100
40	1.0883	0.9811	0.9134	0.9528
60	0.8839	0.9717	0.7418	0.9340
80	0.7564	0.9340	0.6348	0.8962
100	0.6683	0.9783	0.5609	0.9565

Table 4. ALCIs and CPs for $\lambda = 0.5$.

n	95% ACI		95% CRI	
	ALCI	CP	ALCI	CP
20	0.3399	0.9520	0.2852	0.9110
40	0.2458	0.9340	0.2063	0.8868
60	0.2022	0.9340	0.1697	0.8868
80	0.1733	0.9245	0.1455	0.8868
100	0.1572	0.9348	0.1319	0.9348

Tracing plots of the posterior samples of the parameter λ in Figure 3 and the parameter k computed using the Metropolis-Hastings algorithm are shown in Figure 4. These graphs show well-mixed chains with steady variations and no visible trends, suggesting satisfactory convergence and accuracy of the provided Bayesian estimates.

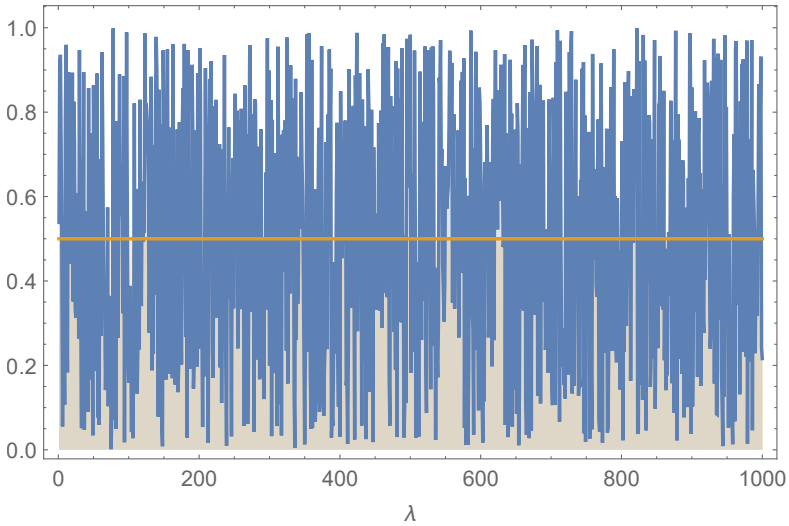

Figure 3. Tracing plot for the parameter λ.

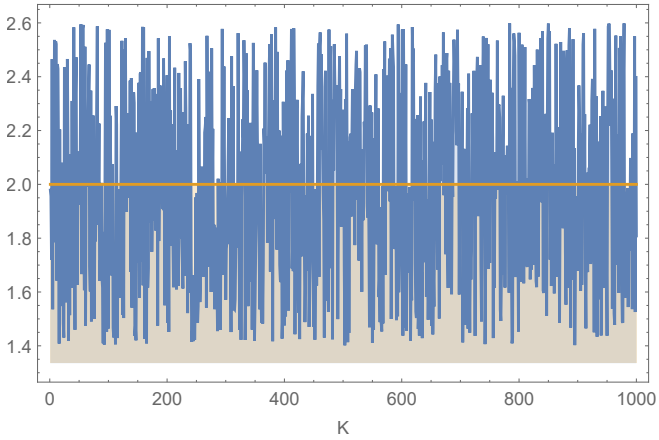

Figure 4. Tracing plot for the parameter k.

Figure 5 shows the autocorrelation function (ACF) of the MCMC samples, supplementing the trace plots of Figures 3 and 4. The fact that the autocorrelation decays rapidly as lag increases implies that successive samples are not correlated too strongly, and therefore the Markov chains are likely to be mixed efficiently. This, combined with the good trace plots, further indicates good convergence and justifies the trustworthiness of the Bayesian estimates obtained based on the Metropolis-Hastings algorithm.

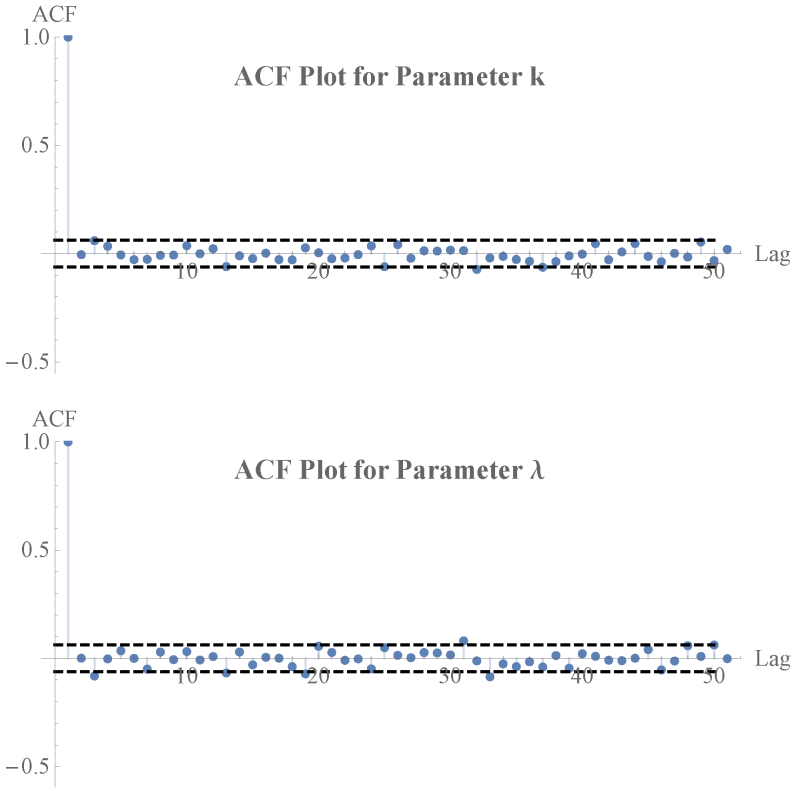

Figure 5. ACF for the parameters k and λ.

From Tables 1–4, it is noted that:

(1) Tables 1 and 2 show that the MSEs for the parameters k and λ consistently decrease across all estimation methods (MLE, SEL, LINEX) as sample size (n) increases. This demonstrates that larger samples yield more precise and reliable point estimates, reflecting the consistency property of the estimators.
(2) According to Tables 1 and 2, for both parameters, the Bayesian estimates under SEL usually reveal the smallest MSE values when compared to MLE and LINEX, especially for smaller sample sizes (e.g., $n = 20$ and 40). This implies that the Bayesian technique yields more effective estimates than maximum likelihood for this model when the informative priors are given.
(3) Tables 3 and 4 demonstrate that the asymptotic confidence intervals (ACIs) based on MLE are consistently larger than the credible intervals (CRIs) derived using the MCMC approach. This implies that the Bayesian technique provides interval estimates that are more precise.
(4) Tables 3 and 4 demonstrate that the MCMC CRIs typically offer coverage probabilities (CPs) that are closer to the 95 percent level than the asymptotic MLE intervals (ACIs). The MLE-based intervals, for instance, differ more for $n = 20$ than the CRI, which has a CP of 0.9520 for k and 0.9110 for λ. This demonstrates how small samples improve the performance of the Bayesian intervals and shows how the Bayesian intervals perform better in small samples.

6. Application to real data

This section offers a real data set as an actual instance to demonstrate how the methods proposed in this paper can be applied to the data in this scenario. The data, which were initially published in Aarset [3] and Gonzalez et al. [4], comprise the failure times of 50 devices that were put through a life test starting at $y = 0$. The observed lifetimes are summarized below:
0.1, 0.2, 1, 1, 1, 1, 1, 2, 3, 6, 7, 11, 12, 18, 18, 18, 18, 18, 21, 32, 36, 40, 45, 46, 47, 50, 55, 60, 63, 63, 67, 67, 67, 67, 72, 75, 79, 82, 82, 83, 84, 84, 84, 85, 85, 85, 85, 85, 86, 86.

Because the theoretical support for the UASWD is restricted to the open unit interval $(0, 1)$, the raw observations had to be transformed before the model could be estimated. Using a min–max normalization, we represented the data onto the [0, 1] range:

$$y_i^* = \frac{y_i - min(y)}{max(y) - min(y)}, \qquad i = 1, 2, ..., n. \tag{6.1}$$

Any boundary values resulting from the transformation (0 or 1) were excluded for consistency with the distribution's support. In addition to making accurate inference easier, this linear rescaling preserves the fundamental stochastic structure and relative ordering of the observations. The normalized dataset used in the analysis is as follows:

0.00116	0.01048	0.01048	0.01048	0.01048	0.01048	0.02212	0.03376	0.06868
0.08033	0.12689	0.13853	0.20838	0.20838	0.20838	0.20838	0.20838	0.24331
0.37136	0.41793	0.46449	0.52270	0.53434	0.54598	0.58091	0.63912	0.69732
0.73225	0.73225	0.77881	0.77881	0.77881	0.77881	0.83702	0.87194	0.91851
0.95343	0.95343	0.96508	0.97672	0.97672	0.97672	0.98836	0.98836	0.98836
0.98836	0.98836							

The Kolmogorov-Smirnov $(K - S)$ test performed on the data revealed that the distance equals 0.0917171 and the p-value equals 0.790246; see Figure 6.

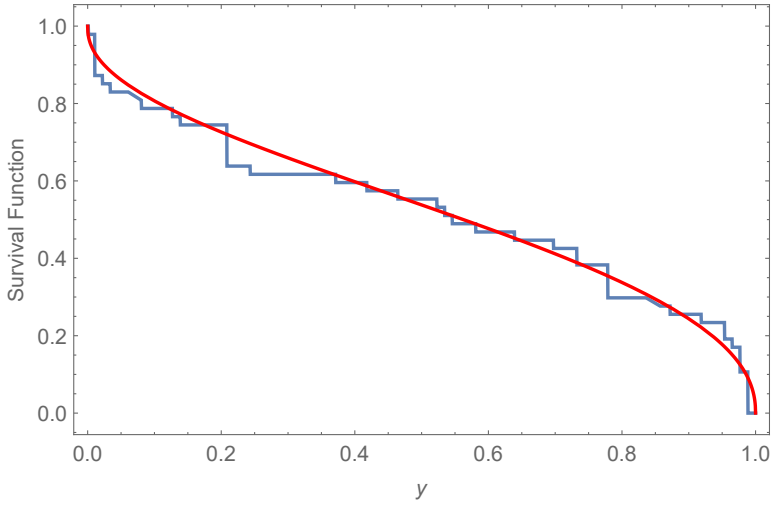

Figure 6. K-S test shows that UASWD is well-fitted to the observed data set.

In Figure 5, the fitted survival function of the UASWD (smooth red curve) is plotted against the empirical survival function (stepwise blue curve). The suggested model offers a sufficient representation of the observed data, as evidenced by the strong agreement between the two curves over the entire support.

From Table 5, it is noted that:

(1) The MLEs for both parameters ($k = 0.9952, \lambda = 0.9716$) are significantly lower than the Bayesian estimates (ranging from 1.68 to 1.73), indicating that the informative priors strongly influence the posterior estimates. Additionally, Bayesian credible intervals are narrower than MLE confidence intervals, demonstrating higher precision.

(2) The Bayesian estimates demonstrate stability and minimal variation, indicating a symmetric posterior distribution. The strong model fit (K-S test p-value = 0.7902) further confirms the reliability of the Bayesian method for this dataset.

Table 5. Different point estimates for k and λ, 95% CI and 95% CRIs.

Parameter	Method	Estimated Value	Parameter	Estimated Value
k	MLE	0.9952	λ	0.9716
	SEL	1.7004		1.7096
	LINEX ($c = -2$)	1.7191		1.7316
	LINEX ($c = 2$)	1.6828		1.6801
	95% CI	[0.74846, 1.24196]	95% CI	[0.51836, 1.42492]
	Length	0.906559	Length	0.91084
	95% CR	[1.4239, 2.0354]	95% CR	[1.2665, 1.9051]
	Length	0.61155	Length	0.638603

The maximum likelihood (ML) approach is now used to estimate the unknown parameter of the UASED. Four different unit distributions, the unit-Weibull distribution (UWD) defined by Mazucheli

et al. [5], the UIWD, suggested by Ribeiro-Reis [6], the transmuted unit distribution (TUD), discussed by Shaw and Buckley [14], and the unit power distribution (UPD) reviewed by Ahsanullah [15], were fitted to the same normalized dataset for comparative analysis. The same numerical optimization techniques and convergence criteria were applied to all models in order to provide methodological coherence and an equitable foundation for comparison.

The ML estimates, the related standard errors (S.E.), the values of -2 times the maximal log-likelihood ($-2l$), and a set of penalized likelihood-based model selection criteria are shown in Table 6. The Akaike information criterion (AIC), the consistent Akaike information criterion (CAIC), the Bayesian information criterion (BIC), and the Hannan–Quinn information criterion (HQIC) were used to assess the model's adequacy. Table 6 shows the ML estimates and their related values. Additionally, it reports empirical distribution function measurements, specifically the Anderson–Darling (A^*), Cramér–von Mises (W^*), and Kolmogorov–Smirnov (K–S) statistics, along with the corresponding K–S test p-values, for further diagnostic examination.

According to numerical results in Table 6, the UASWD achieves the lowest values for each of the information criteria that were taken into consideration (AIC, CAIC, BIC, and HQIC). In penalized likelihood frameworks, this implies that the UASWD provides the most effective trade-off between model complexity and quality of fit. Additionally, at standard significance levels, the UASWD produces the greatest K-S p-value (0.7902), indicating no statistically significant difference between the actual and theoretical distributions

Table 6. ML estimates with different goodness-of-fit results for failure-time data.

Model	UASWD (k, λ)	UWD (λ, θ)	UIWD (λ, θ)	TUD (λ)	UPD (λ)
Est.	0.9952, 0.9716	0.9989, 0.6408	0.3746, 0.5067	-0.0800	0.7414
S.E.	0.2467, 0.4533	0.1535, 0.0756	0.0809, 0.0550	0.1961	0.1081
-2ℓ	-22.2789	-21.9090	-6.8715	-0.1657	-4.6601
AIC	-20.2789	-17.9090	-2.8715	1.8343	-2.6601
CAIC	-20.1901	-17.6363	-2.5988	1.9232	-2.5713
BIC	-18.4288	-14.2087	0.82880	3.68440	-0.81000
HQIC	-19.5827	-16.5166	-1.4791	2.5305	-1.9639
A^*	0.758470	0.66970	1.96770	5.70620	6.21510
W^*	0.0491221	0.07810	0.31510	0.48520	0.66710
K-S	0.0917171	0.10160	0.17160	0.18390	0.21920
P-value	0.790246	0.67950	0.11120	0.07290	0.10830

7. Conclusions

In this paper, a new two-parameter distribution on the unit interval (0, 1) that can be used to model bounded lifetime and reliability data was proposed. The model has a flexible hazard rate behavior, including a bathtub-shaped, and presents explicit statements of structurally important properties.

Both maximum likelihood estimation and Bayesian estimation procedures were established, and the performance of the estimators was satisfactory, with the results of the simulation showing better performance in small samples by Bayesian methods.

The model was implemented using the normalized life-testing experiment data of 50 devices on

failure time. The goodness-of-fit metrics indicated that the given distribution fits much better than a number of existing unit models. The model is suggested, based on these results, to be reliable in the analysis of limited or normalized lifetime data, especially in the presence of complicated structures of hazards.

On the basis of these findings, we suggest the proposed model for analyzing bounded lifetime data, particularly in the reliability situation where the hazard rates are bathtub-shaped. The Bayesian estimation process proves especially useful in cases where the sample sizes are small because it will give more stable and accurate interval estimates.

In summary, the suggested framework combines analytic tractability, inferential robustness, and practical applicability, and thus it is a valuable addition to the category of unit-interval lifetime distributions.

Author contributions

Naelah Alghufily: Methodology, validation, resources, writing – review & editing, funding acquisition; Khalaf S. Sultan: Methodology, conceptualization, formal analysis, investigation, supervision; Mahmoud M. M. Mansour: Methodology, validation, data curation, visualization; Nagwa M. Mohamed: Methodology, conceptualization, software, investigation, resources, writing – original draft preparation. All authors have read and approved the final version of the manuscript for publication.

Use of Generative-AI tools declaration

The authors declare they have not used Artificial Intelligence (AI) tools in the creation of this article.

Funding

This research was funded by Researchers Supporting Project number (PNURSP2026R523), Princess Nourah bint Abdulrahman University, Riyadh, Saudi Arabia.

Conflicts of interest

The authors declare no conflicts of interest.

References

1. J. Mazucheli, A. F. B. Menezes, L. B. Fernandes, R. P. de Oliveira, M. E. Ghitany, The unit-Weibull distribution as an alternative to the Kumaraswamy distribution for the modeling of quantiles conditional on covariates, *J. Appl. Stat.*, **47** (2019), 954–974. http://dx.doi.org/10.1080/02664763.2019.1657813
2. L. Tierney, Markov chains for exploring posterior distributions, *Ann. Statist.*, **22** (1994), 1701–1728. http://dx.doi.org/10.1214/aos/1176325750

3. M. V. Aarset, How to identify a bathtub hazard rate, *IEEE Trans. Reliab.*, **R-36** (1987), 106–108. http://dx.doi.org/10.1109/TR.1987.5222310
4. I. J. González-Hernández, L. C. Méndez-González, R. Granillo-Macías, J. L. Rodríguez-Muñoz, J. S. Pacheco-Cedeño, A new generalization of the uniform distribution: Properties and applications to lifetime data, *Mathematics*, **12** (2024), 2328. http://dx.doi.org/10.3390/math12152328
5. J. Mazucheli, A. F. B. Menezes, M. E. Ghitany, The unit-Weibull distribution and associated inference, *J. Appl. Probab. Stat.*, **13** (2018), 1–22.
6. L. D. Ribeiro-Reis, The unit inverse Weibull distribution and its associated regression model, *J. Econom. Stat.*, **3** (2023), 55–68. https://doi.org/10.47509/JES.2023.v03i01.04
7. R. Xing, The application of coefficient of variation estimation in reliability study of existing structure, In: *2018 2nd IEEE advanced information management, communicates, electronic and automation control conference (IMCEC)*, 2018, 2652–2657. https://doi.org/10.1109/IMCEC.2018.8469617
8. N. Kumar, A. Dixit, V. Vijay, Entropy measures and their applications: A comprehensive review, *arXiv:2503.15660*, 2025. https://doi.org/10.48550/arXiv.2503.15660
9. B. C. Arnold, N. Balakrishnan, H. N. Nagaraja, *A first course in order statistics*, 2008. https://doi.org/10.1137/1.9780898719062
10. N. U. Nair, P. G. Sankaran, N. Balakrishnan, *Reliability modeling and analysis in discrete time*, Academic Press, 2018. https://doi.org/10.1016/C2014-0-01528-6
11. R. L. Burden, J. D. Faires, A. M. Burden, *Numerical analysis*, 10 Eds., Cengage Learning, 2015.
12. A. C. Cohen, Maximum likelihood estimation in the Weibull distribution based on complete and on censored samples, *Technometrics*, **7** (1965), 579–588. http://dx.doi.org/10.1080/00401706.1965.10490300
13. H. R. Varian, A Bayesian approach to real estate assessment, In: *Studies in Bayesian econometrics and statistics*, North-Holland Pub. Co., 1975, 195–208.
14. W. T. Shaw, I. R. C. Buckley, The alchemy of probability distributions: beyond Gram-Charlier expansions, and a skew-kurtotic-normal distribution from a rank transmutation map, *arXiv:0901.0434*, 2009. https://arxiv.org/abs/0901.0434 .
15. M. Ahsanullah, *Handbook on univariate statistical distributions*, Trafford, 2011.